



ORIGINAL RESEARCH ARTICLE

## ANALYSIS OF THE SEASONAL VARIATION IN TURBIDITY INDEX IN SUDAN AND FRESH WATER SWAMP VEGETATION ZONES, NIGERIA

S. U. Muhammad<sup>1\*</sup>, W. C. Solomon<sup>1</sup>, D. B. Yahaya<sup>2</sup>, and J. S. Enaburekhan<sup>2</sup>

<sup>1</sup>Department of Mechanical Engineering, Nigerian Defence Academy, Kaduna State, Nigeria

<sup>2</sup>Department of Mechanical Engineering, Bayero University, Kano State, Nigeria

\*Corresponding author's email address: [sumuhammed@nda.edu.ng](mailto:sumuhammed@nda.edu.ng)

### ARTICLE INFORMATION

Submitted 20 February, 2021

Revised 8 June, 2021

Accepted 12 June, 2021

### Keywords:

Linke turbidity  
Angstrom turbidity  
meteorological data  
Sudan vegetation  
fresh water swamp  
vegetation

### ABSTRACT

This study evaluates the seasonal turbidity index of two vegetation zones in Nigerian which are Sudan and Fresh water swamp. Thirty years (1981 – 2010) meteorological data of temperature, relative humidity and solar radiation were obtained from the archives of the Nigerian Meteorological agency (NIMET). Annual and monthly analysis of the turbidity coefficients were mainly based on the Linke and Angstrom methods, due to absence of radiosonde data. The results show that the monthly mean values of the clear-sky global radiation lies between 19.34 MJ/m<sup>2</sup>day to 24.44 MJ/m<sup>2</sup>day (for Sudan vegetation) and 15.54 MJ/m<sup>2</sup>day to 20.28 MJ/m<sup>2</sup>day (Fresh water swamp). Meanwhile, the monthly percentages of clearness index above 0.6 were estimated as 75% and 33.3, and for the water vapour content exceeding 3 cm to be 58.3% and 100%, for the Sudan and Fresh swamp vegetation, respectively. These values contribute significantly to the reduction of direct radiant energy. The results obtained for the seasonal index for Linke and Angstrom coefficients show that for the wet season, the index exceeded the dry value by 25.99% and 23.66% for Sudan and Fresh swamp vegetation, respectively. By implication, the Fresh water Swamp is laden with more aerosols than Sudan zone. Additionally, the R<sup>2</sup> obtained for the relationship between Angstrom and Linke is 0.999 for both locations. Hence, the study provides an insight into the contribution of aerosol in the attenuation of solar radiation over the atmosphere for these locations.

© 2021 Faculty of Engineering, University of Maiduguri, Nigeria. All rights reserved.

### 1.0 Introduction

Solar radiation measurements and or estimations from models that employed meteorological parameters, under clear skies (or cloudless skies), for the purpose of designing solar equipment for optimal performance, with the view of establishing the viability of solar components in Nigeria. Solar energy is one of the key renewable energies available (Oyepedo, 2012). But in Nigeria, the major source of energy comes from fossil fuels (Ogunsola, 1990). The use of these fuels, however, leads to the generation of environment problems such as air pollution, greenhouse gases (GCGs), and aerosol production (Marif et al., 2018). The presence of these aerosol particles in the atmosphere could be as a result of natural phenomenon (e.g. dust or storm). In addition to this aerosol, the atmosphere consists of other gases, which remain constant while the water moisture content varies with season. Hence, as radiant energy passes through the atmosphere, it comes in contact with these components, which tend to reduce the intensity of the radiant heat, from the sun through scattering or absorption (Marif et. al., 2017).

Therefore, atmospheric turbidity could be described as the main parameter controlling the attenuation of solar radiation reaching the earth's surface under clear sky conditions, which equally serves as a tool for assessing air pollution of any particular area. Continues alteration of

atmosphere due to human activities causes an increase in aerosol concentration level which has a significant impact on the environment and radiant energy at the earth's surface.

Although, turbidity can be obtained directly from observation performed during clear sky periods, few stations are available in Africa, such as Nigeria, where turbidity is measured as highlighted (Diabte et al., 2003; Oba et al., 2016). Hence, the study of atmospheric turbidity is important in estimating the actual solar irradiance on the earth's surface. It has become important parameter, especially, in the area of evaluation solar energy appliances and also for the determination of the amount of spectral global irradiance for the photovoltaic cells designing and for the selective absorber for spectral thermal collectors. In the present study Sokoto and Kano were used as sampling stations to represent Sudan vegetation, while PortHarcourt to represent fresh water swamp vegetation, to estimate the seasonal variation in turbidity. Several literatures on measurement and estimation of turbidity exist (Canada et al., 1992; Cucumo et al., 2000; Hemdy et al., 2001; Power, 2001; Lopez et al., 2004; Oba et al., 2016; Ambaye et al., 2018). However, two major indices of turbidity are the Linke turbidity factor ( $T_L$ ), and the Angstrom turbidity coefficient ( $\beta$ ). Both are used to quantify the influence of atmospheric aerosols on direct solar radiation on earth's surface.

The objectives of this article are to report data on aerosol optical depth and atmospheric turbidity coefficients with the view to investigating the seasonal variation in turbidity as a result of changes in the atmospheric meteorological parameters for the two different vegetation zones in Nigeria, which are on Sudan (short grass savanna) and fresh water swamp vegetations.

## 2 Materials and Methods

### 2.1 Study area

Federal republic of Nigeria lies in the western part of Africa. It consists of seven major vegetation zones as shown in Figure I. The Stations selected from the Sudan vegetation zone are Sokoto and Kano while station selected from the Fresh Water Vegetation zone is Port-Harcourt, for the current study. The details of each station are presented in Table I

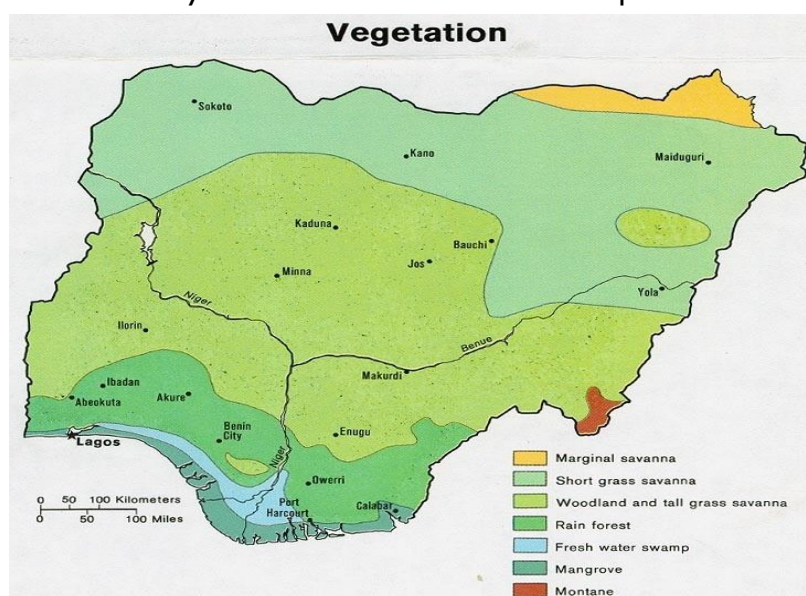


Figure I: Vegetation map of Nigeria (F.G.N. 2002)

**Table I:** Geographical locations of selected areas

Station	Longitude (°N)	Latitude (°E)	Height (m.a.s.l)	Year
Kano	8.53	12.05	714	1982 – 2010
Sokoto	5.25	13.02	350.75	1982 – 2010
Port-Harcourt	7.02	4.85	195.51	1982 – 2010

The Sudan Vegetations are semi-desert, with minimal rainfall, supports a mixture of grasses and acacia scrub while fresh water swamps vegetations zones are usually endemic where the most significant part of forests occur. Hence, the two vegetation zones are located areas characterized by different weather conditions as indicated in Figure 1. Therefore, the data used in this study were obtained from Nigerian Meteorological Agency (NIMET), from 1981 to 2010. Daily record of weather parameters used includes temperature, solar radiation and relative humidity. The daily weather parameters were converted into mean monthly values.

## 2.2 Theory

Linke's turbidity factor,  $T_L$ , is an index of the number of clear dry atmosphere that would be necessary to produce attenuation of the extraterrestrial radiation that is produced by the real atmosphere. In this study, the Linke turbidity was estimated using the empirical equation proposed by Dogniaux (Dogniaux, 1974). The estimation involves using inputs of solar elevation ( $\alpha$ ) (in degrees), precipitable water  $\omega$  (in cm), and Angstrom's turbidity  $\beta$ .

The empirical relationship between Linke and Angstrom is expressed as:

$$T_L = \left( \frac{85 + \sin \alpha}{39.5e^{-\omega} + 47.4} + 0.1 \right) + (16 + 0.22\omega)\beta \quad (1)$$

However, the Linke turbidity factor is related to measures of direct irradiance,  $I_d$ , by means of the following equation as:

$$T_L = \frac{1}{\delta_R m_a} \ln \left( \frac{I_o}{I_b} \right) \quad (2)$$

where:  $\delta_R$  is the Rayleigh optical thickness,  $\alpha$  is the altitude angle (degree),  $\omega$  precipitable water content in the atmosphere (cm),  $\beta$  is Angstrom's turbidity,  $T_L$  Linke turbidity factor,  $m_a$  relative optical air mass,  $I_o$  is the extraterrestrial normal irradiance ( $W/m^2$ ),  $I_b$  is the beam radiation ( $W/m^2$ ).

However, details on the analysis of solar radiation components for the specific locations were documented elsewhere (Muhammad et al., 2016). However, the clear-sky global radiation,  $H_f$  ( $MJ/m^2/day$ ) at the surface was estimated using the model proposed by Kondo, Nakamura and Yamazaki (Kondo et al., 1991).

$$\frac{H_f}{H_o} = (C_1 + 0.7 \times 10^{-m_d F_1})(1 - i_3)(1 - j_i) \quad (3)$$

Where  $H_o$  is the monthly mean global solar radiation at the top of the atmosphere  
 $C_1 = 0.21 - 0.2\beta_{Dust}$ , ( $\beta_{Dust} < 0.3$ ) (3a)

$$C_1 = 0.15, \quad (\beta_{\text{Dust}} \geq 0.3) \quad (3b)$$

$$m_d = k_3 m_{\text{NOON}} \quad (3c)$$

$$m_{\text{NOON}} = \left(\frac{P}{P_0}\right) \sec(\varphi - \delta), \quad (\varphi - \delta < \pi/2) \quad (3d)$$

$$m_{\text{NOON}} = \alpha, \quad (\varphi - \delta \geq \pi/2) \quad (3e)$$

$$k_3 = 1.402 - 0.06 \log_{10}(\beta_{\text{Dust}} + 0.02) - 0.1[\sec(\varphi - \delta) - 0.91]^{1/2} \quad (3f)$$

$$F_1 = 0.056 + 0.16 (\beta_{\text{Dust}})^{1/2} \quad (3f)$$

$$i_3 = 0.014 (m_d + 7 + 2 \log_{10} \omega) \log_{10} \omega \quad (3h)$$

$$j_i = \left[0.066 + 0.34 (\beta_{\text{DUST}})^{1/2}\right] (\text{ref} - 0.15) \quad (3i)$$

$m_d$  = daily – mean path length (dimensionless)

ref = albedo (dimensionless)

$i_3$  = Julian day

For the Linke turbidity factor, the determination of  $\bar{\delta}_R$  is based on improved Kasten formula for Rayleigh optical thickness (Kasten, 1996), which actually depends only on the relative air mass values. The expression of  $\bar{\delta}_R$  is defined by the expression:

$$\delta_R = \frac{1}{6.6296 + 1.7513m_a - 0.1202m_a^2 + 0.0065m_a^3 - 0.00013m_a^4}, \quad m_a \leq 20 \quad (4)$$

$$\text{Or } \delta_R = \frac{1}{10.4 + 0.718m_a}, \quad m_a > 20 \quad (5)$$

However, the relative optical air mass at standard condition (Kasten, 1996), dependent on the corrected solar altitude and the correction for a given elevation (height above sea level) in a relation expressed (Lopez et al., 2004) and (Becker, 2001), respectively.

$$m_a = \frac{P}{P_0} \frac{1}{\sin \alpha^c + 0.50572(\alpha^c + 6.07995)^{-1.6364}} \quad (6)$$

$$\alpha^c = \alpha + 0.61359 \frac{0.1594 + 1.123\alpha + 0.06565\alpha^2}{1 + 28.9344\alpha + 277.3971\alpha^2} \quad (7)$$

$$\frac{P}{P_0} = 10(\text{height above sea level}/18400 \times (1 + 0.004T_{\text{air}})) \quad (8)$$

where  $\alpha^c$  Altitude angle

$T_{\text{air}}$  is air temperature in degree Celsius

$P_0$  is the surface air pressure (1023.25hPa)

Details of analysis and the results of precipitable water content have been documented elsewhere (Muhammad et al., 2016b).

### 3 Results and Discussion

The monthly and annual mean values of the estimated parameters are presented in Tables 2 and 3. The monthly mean global solar radiation at the top of the atmosphere ( $H_0$ ) varies from 31.06 to 41.68 (MJ/m<sup>2</sup>day) and 34.91 to 40.4 (MJ/m<sup>2</sup>day) for Sudan and Fresh Water Swamp zones, while annual mean values of 37.874 (MJ/m<sup>2</sup>day) and 38 544 (MJ/m<sup>2</sup>day), respectively.

However, the estimated annual mean values for the sky-clear global radiation at the surface of the earth were found to be 21.776 and 18.136 for Sudan and Fresh Water Swamp zones, respectively.

**Table 2:** Sudan Vegetation zone

Month	$H_o$ (MJ/m <sup>2</sup> day)	$H_f$ (MJ/m <sup>2</sup> day)	$K_t$	$H_b$ (%)	$\omega$ (cm)	$m_a$	$\bar{\delta}_r$
January	31.97	21.3	0.664	0.75	1.32	6.685	0.069
February	35.34	23.45	0.664	0.75	1.49	5.659	0.073
March	38.64	24.69	0.636	0.73	1.61	4.723	0.078
April	40.97	24.44	0.61	0.71	3.05	4.164	0.082
May	41.66	22.58	0.536	0.66	4.3	4.257	0.081
June	41.65	21.26	0.526	0.65	4.61	4.512	0.08
July	41.68	19.65	0.477	0.61	4.74	4.501	0.08
August	41.45	19.34	0.466	0.6	4.8	4.237	0.081
September	39.95	20.28	0.499	0.63	4.7	4.516	0.08
October	36.92	21.69	0.594	0.7	3.42	5.162	0.076
November	33.2	21.96	0.658	0.75	1.79	6.158	0.071
December	31.06	20.67	0.656	0.75	1.75	6.903	0.068
<b>Mean Value</b>	<b>37.874</b>	<b>21.776</b>	<b>0.582</b>	<b>0.691</b>	<b>3.132</b>	<b>5.123</b>	<b>0.077</b>

**Table 3:** Fresh water swamp vegetation zone

Month	$H_o$ (MJ/m <sup>2</sup> day)	$H_f$ (MJ/m <sup>2</sup> day)	$K_t$	$H_b$ (%)	$\omega$ (cm)	$m_a$	$\bar{\delta}_r$
January	35.590	20.120	0.567	0.680	4.720	2.713	0.094
February	37.930	21.030	0.556	0.670	5.280	2.381	0.098
March	39.800	20.280	0.507	0.630	5.710	2.093	0.102
April	40.400	19.330	0.482	0.610	5.790	2.040	0.103
May	39.730	18.300	0.464	0.600	5.710	2.253	0.100
June	39.030	16.620	0.429	0.560	5.480	2.412	0.098
July	39.310	15.540	0.377	0.510	5.300	2.375	0.098
August	40.170	15.580	0.380	0.510	5.220	2.186	0.101
September	40.290	16.680	0.416	0.550	5.370	2.014	0.103
October	38.900	17.340	0.448	0.580	5.430	2.253	0.100
November	36.470	17.880	0.492	0.620	5.500	2.577	0.096
December	34.910	18.930	0.549	0.670	5.030	2.796	0.093
<b>Mean Value</b>	<b>38.544</b>	<b>18.136</b>	<b>0.472</b>	<b>0.599</b>	<b>5.378</b>	<b>2.341</b>	<b>0.099</b>

Therefore, it may be inferred from the results above that solar radiation availability is a function of region, season and day of the year i. e., the day-to-day variability of extraterrestrial radiation could be attributed to cloud effects and the distance between the sun and the location. In essence, locations that are located at the upper level of the northern hemisphere tend to have more radiation at the top than those at the bottom. This implies that the rainy season corresponds to period of high radiation at the top of the atmosphere.

From the analysis of the diffuse and clearness index carried out, it is very clear that the contribution of fraction of diffuse component of solar radiation is very low throughout the year with the exception of the monsoon period (peak of rainy season) i.e. from the months of May to September for Sudan vegetation and May to October for fresh water swamp vegetation zones. It could be inferred from the results that visibility of the atmosphere is a function of the amount of beam radiant energy received for a given location. The higher the beam radiation the more the clearness index. Hence, the variability of the clearness index is dependent on the season of the year. Clearly, the atmosphere above fresh water swamp vegetation zone is laden with high moist content couple with industrial activities. This signifies low clearness index, whereas the Sudan vegetation zone indicates high clearness index in all season.

The water vapour content in the atmosphere also plays a vital role in the attenuation of the incoming radiant energy. High content of water vapour was observed to occur in the fresh water swamp zone, with low percentage recorded in the Sudan zone. This could be attributed to the fact that the location of the former zone is prone to high moisture content than the latter (Sudan). This parameter contributes significantly in the absorption of the incoming radiant energy, before it arrives at the earth surface. That is why, Sudan zone recorded high beam radiation than the fresh water swamp.

The seasonal values of Linke Turbidity factor ( $T_L$ ) and Angstrom coefficient ( $\beta$ ) were all presented in Tables 4 and 5, respectively. It is clear that Sudan vegetations have low  $T_L$  and  $\beta$  values in comparison with fresh water swamp zone. This could be as a result of the latter being at lower altitude than the former. The  $T_L$  values for the different vegetation zones offer a wide range of values (2.77 to 8.004) and exhibits the same dynamics (the same trend): the values increased from January to August and decreased from September to December, with maximum attained values in August. These variations may also equally be related to the local climates.

**Table 4:** Seasonal Index Factor for Wet Season (April-September)

Months	Linke Turbidity ( $T_L$ )		Angstrom coefficient ( $\beta$ )	
	Sudan Vegetation	Fresh water swamp vegetation	Sudan Vegetation	Fresh water swamp vegetation
April	3.862	7.117	0.120	0.301
May	4.083	6.817	0.129	0.284
June	3.983	6.927	0.122	0.291
July	4.257	7.799	0.138	0.342
August	4.519	8.193	0.153	0.365
September	4.128	8.004	0.130	0.354
<b>Average</b>	<b>4.139</b>	<b>7.476</b>	<b>0.132</b>	<b>0.323</b>

**Table 5:** Seasonal Index Factor for Dry Season (October-March)

Months	Linke Turbidity ( $T_L$ )		Angstrom coefficient ( $\beta$ )	
	Sudan Vegetation	Fresh water swamp vegetation	Sudan Vegetation	Fresh water swamp vegetation
October	3.428	7.016	0.093	0.296
November	2.911	6.032	0.075	0.239
December	2.736	5.335	0.067	0.200
January	2.777	5.347	0.073	0.203
February	3.059	5.895	0.089	0.232
March	3.467	6.767	0.108	0.281
<b>Average</b>	<b>3.063</b>	<b>6.065</b>	<b>0.084</b>	<b>0.242</b>

From November to February, the Sudan zone, experience full dry/cool season laden with harmattan dust, hot/dry season from March to May, and rainy season from June to September which constitute high volume of water moisture. Whereas the fresh water swamp vegetation zones comprise of warm moist air from Atlantic Ocean with high volume of pollution from traffic and industries (mostly loaded with petrochemical companies) during the wet season. Likewise, the Angstrom turbidity ( $\beta$ ) values exhibit the same evolutions in  $T_L$ , with values increasing from January to August and while experiences a decrease from September to December. The high values are equally due to higher average precipitable water in the air. Hence, from the month of May to October, fresh water swamp tends to have the most polluted atmosphere whereas Sudan zone possess a combination of clear/warm air and moist/warm air. Therefore, from the foregoing, fresh water swamp vegetation zones are more turbid (polluted) then followed by Sudan vegetation.

In addition, from Table 4, the seasonal index factor for wet season falls averagely between 4.139 and 7.479 for Sudan and Fresh water swamp zones which could be classified as moist/warm air and polluted atmosphere, respectively. On the other hand, from Table 5, the seasonal index for dry values 3.06 (for Sudan) and 6.065 (Fresh water swamp) could be classified as clear/warm air and moist/warm (or polluted) air, respectively (Scharmer and Grief. 2000).

Hence, it could be inferred, from above, that the  $T_L$  index of the number of clear dry that gave rise to attenuation of the extraterrestrial radiation atmosphere, for both seasons, was highest for Fresh water swamp zone than the Susan Zone. Therefore, the Fresh water swamp zone has the tendency to produce more extinction than the Sudan zone, as a result of presence of more water content in the atmosphere. Also, the  $T_L$  indexes are generally affected by the atmospheric water content, since considerable percentage of aerosol particle in the atmosphere are hygroscopic in nature. As such, some of the aerosol particles, present in the atmosphere have tendency to absorb moisture which results in the variation/change in shape of the particle. Hence, the Linke turbidity index could be adopted as a reasonable quantity to measure he turbidity of a local environment.

Moreover, the Angstrom Coefficient, which is dimensionless, varies between 0.00 and 0.5 for an atmosphere that is completely cleaned and that with a very high aerosol amounts,

respectively (Hemdy et al., 2001). The analysis of the values for the Sudan zone showed that about 41.67% of the Angstrom coefficient range between 0.02 and 0.1, 50% are between 0.1 and 0.2 and 8.33% exceed 0.15. While for the Fresh water swamp zone, about 66.67% of the Angstrom coefficient ranged between 0.2 and 0.3 and 33.33% exceed 0.3. In terms of wet seasonal variation, in the Sudan zone, about 83.33% of the Angstrom coefficient ranged between 0.1 and 0.15 and 16.67% exceed 0.15. on the other hand, in Fresh Water swamp zone, about 66.67% of the values are less than 0.3 and 33.33% are greater than 0.3. In the other hand, in the dry season, results showed that in the Sudan zone, about 83.33% of the values of the Angstrom coefficient are ranged between 0.02 and 0.1 and 16.67% exceed 0.1, while for Fresh Swamp Water zone, about 66.67% of the values ranged between 0 and 0.25 and 33.33% are greater than 0.25.

Tables 4 and 5 shows the results of the seasonal index factor for wet and dry seasons. The Linke turbidity values for fresh water swamp vegetation recorded significant amount for both the dry and wet season. This could be associated with the high moisture content and pollutant originating from petroleum exploration and refining activities, in the atmosphere. Whereas the sudan vegetation zone recorded lower values, except for the months of May to September which correspond with the rainy season in the zone. The climate in the fresh water swamp vegetation zone could be describes as hot/or moist in the dry season while in the wet season as hot/or cool.

Hence, in wet season, fresh water swamp tends to be the most polluted atmosphere, whereas Sudan vegetation possessed combination of clear/warm air and moist/warm air. In dry season, the average values are less than those obtained in summer.

### 3.1 Relationship between Linke factor and Angstrom coefficient

The plot of computed daily average values for Linke Turbidity factor and Angstrom coefficient for the sudan and fresh water swamp vegetation zones, presented in Figure 2 and 3, show a linear relationship. Using a linear regression technique, correlation coefficients of 0.975 and 0.999 were found to exist between the two turbidity factors for Sudan and fresh water swamp, respectively.

$$\text{For sudan vegetation zone:} \quad \beta = 0.045T_L - 0.054 \quad (9)$$

$$\text{Fresh water swamp vegetation zone:} \quad \beta = 0.057T_L - 0.106 \quad (10)$$

Equations 12 and 13 indicate that the linear regression model fitted to  $\beta$  and  $T_L$  for sudan fresh water swamp, are similar to the model reported (Katz et al., 1982 and Eliminir et al., 2001). However, the coefficients of the two models are different from those evaluated elsewhere.



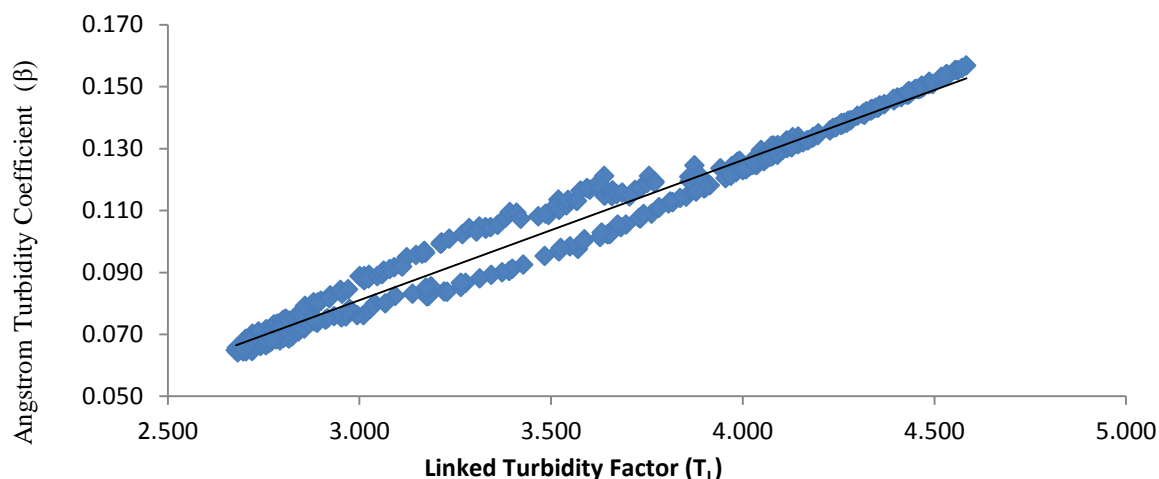


Figure 2: Plots of  $\beta$  versus  $T_L$  Sudan

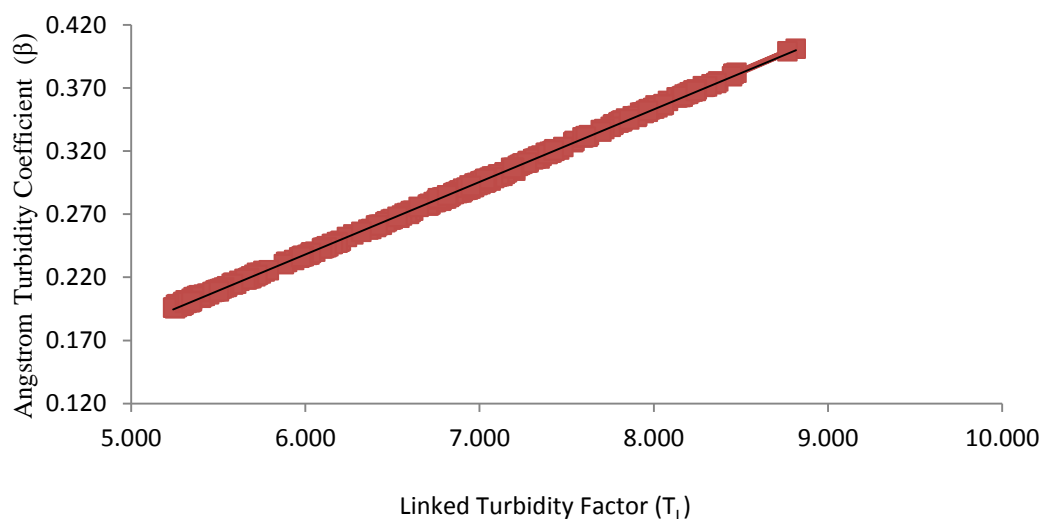


Figure 3: Plot of  $\beta$  versus  $T_L$  Fresh water swamp

### 3.2 Relationship between Angstrom coefficient and precipitable water content

The results of the analysis of precipitable water content and angstrom turbidity coefficient are presented in Figures 4 and 5. For Sudan vegetation zones, from May to November the precipitable water content is higher than the turbidity content of the atmosphere. This is as a result of the fact that, the period represents a combination of seasons with dry/warm air and dry/moist air which is a reflection of high clear index. Hence, graph of Sudan vegetation, turbidity fluctuates with higher values at the beginning of the year, then decreased from the months of April to October and then increased again until the end of the year.

Therefore, for Sudan vegetation where relative humidity and turbidity are low, as solar altitude increased, the increased global solar radiation caused evaporation from soil and rivers which in turn increased precipitable water and forms liquid particles in the atmosphere which contribute to increased turbidity.

The graphs of Figure 5 show the results of precipitable water content and turbidity for fresh water swamp vegetation zones. The graphs show that as precipitable water is higher than turbidity contents with the exception of the months of June, July, August, September and October. The months which corresponds with high turbidity content, represent the peak of

rainy season for the vegetation. Therefore, the presence of excess water vapour with the warm moist air from the Atlantic Ocean account for the high turbidity in these months. Also, from the analysis, it could be inferred that, peak rainy season is always accompanied by the presence of high moisture content in the atmosphere and hence, an increase in turbidity factor.

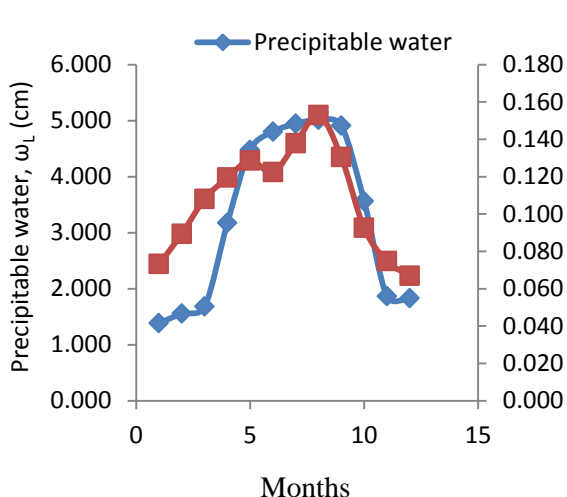


Figure 4: Monthly mean values of turbidity and precipitable water content for Sudan Vegetation

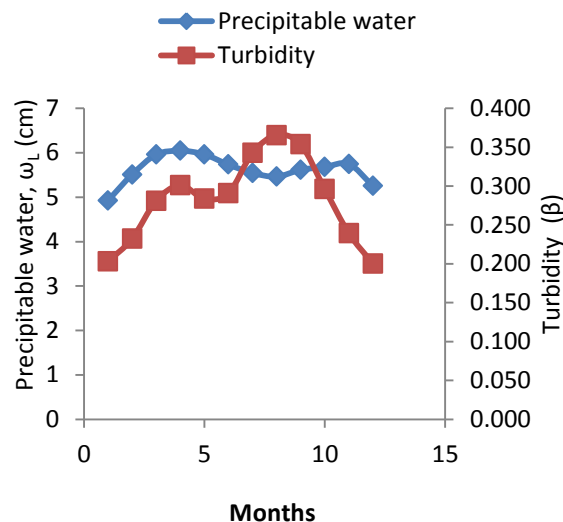


Figure 5: Monthly mean values of turbidity and precipitable water content for Fresh Water Swamp Vegetation

### 3.3 Relationship between Angstrom coefficient and precipitable water

Figures 6 and 7 show the scatter plot of turbidity and precipitable water and the results indicate a linear increase in turbidity with increase in precipitable water content. Using a linear regression technique, models for the computation of  $\beta$  had been developed for the zones with correlation coefficient ranging between 0.160 – 0.750 for fresh water swamp and sudan vegetation zones, respectively. Hence, 75% and 16% of turbidity can be accounted for in the sudan and fresh water swamp vegetation respectively, with respect to known precipitable water content. However, this implies that the statistical relationship between the variables, for fresh water swamp zone, is very weak. It means that only 16% of turbidity can be accounted for using precipitable water content, for this particular zone.

For sudan vegetation zone: 
$$\beta = 0.016\omega + 0.055 \quad (11)$$

For fresh water swamp vegetation zone: 
$$\beta = 0.069\omega - 0.110 \quad (12)$$

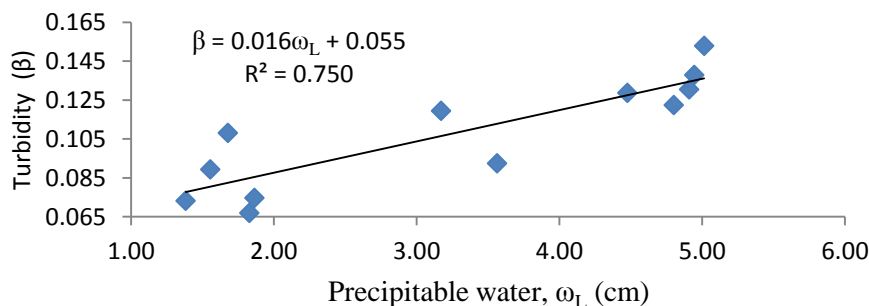


Figure 6: Results of turbidity against precipitable water for Sudan vegetation

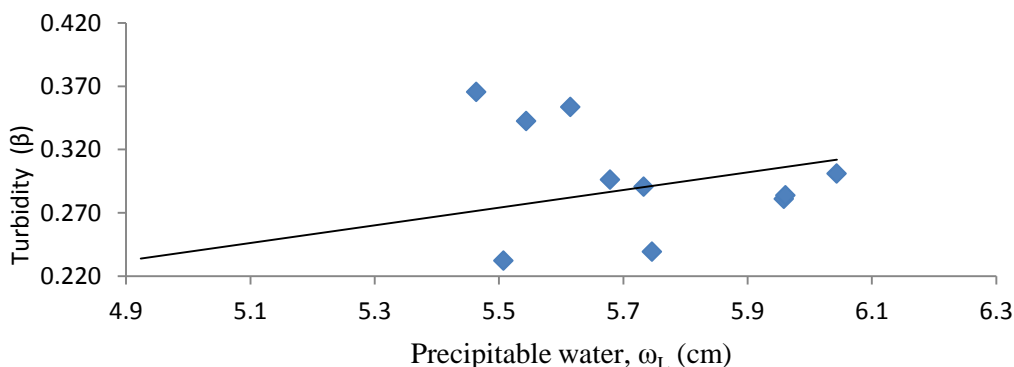


Figure 7: Results of turbidity against precipitable water for Fresh Water Swamp vegetation

#### 4.0 Conclusion

Atmospheric turbidity is often expressed in terms of Linke ( $T_L$ ) and Angstrom factors ( $\beta$ ). In the absence of measured data, the parameters were evaluated based on meteorological data set for two vegetation zones in Nigeria. The results obtained and the statistical evaluation of the data set collected and presented above provide information on the turbidity content in Sudan and fresh water swamp vegetation zones of Nigeria. Thus, the values obtained for the turbidity across the different vegetation zones characterize severe pollution in fresh water swamp than

Sudan vegetation zone. Hence, the obtained values of turbidity and the regression models will serve as reference point in estimating the behaviour of turbidity parameter within the vegetation zones. The variation in the monthly average values of  $T_L$  and  $\beta$  at the two zones show similar trend to those in the literature.

#### References

- Ambaye, C. 2018 Determination of Linke's Turbidity Factor from Model and Measure Solar Radiation in the Tropics Over Highland of South – East Ethiopia. *Journal of Earth Science and Climate Change*, 9(7): 479-483
- Becker, S. 2001. Calculation of Direct Solar Diffuse Radiation in Israel. *International Journal Climatology*, 21 (12): 1561-1576.
- Canada, J. Pinazo, JM. and Bosca, JV. 1992. Determination of Angstrom's Turbidity coefficient at Valencia. *Renewable Energy*, 3 (6-7): 621-626.
- Cucumo, M. Kaliakatsos, D. And Marinelli, V. 2000. A Calculation Method for the Estimation of the Linke turbidity Factor. *Renewable Energy*, 19 (1-2): 249-258.
- Diabate, L., Remund, J. and Wald, L. 2003. Linke Turbidity Factors for Several sites in Africa. *Solar Energy*, 75 (2): 111-119
- Dogniaux, R. 1974. Representation analytique des composantes du rayonnement solaire. *Institute de royal de Meteorologie de Belgique, Serie A 83*: 3-24

Eliminir, HK. Rahama, UA. and Benda, V. 2001. Comparison Between atmospheric Turbidity Coefficients of Desert and Temperate Climates. Acta Polytechnica, 41 (2): 48-59.

FGN. 2002. Atlas of Nigeria. Federal Government of Nigeria

Hamdy, KE. Rahum, UA. and Benda. V. (2001). Comparison Between Atmospheric Turbidity Coefficients of Desert and Temperate Climate. Acta Polytechnica, 41: 48 - 59

Lopez, G. and Batilles, FJ. 2004. Estimate of the Atmospheric Turbidity from Three Broad-Band Solar radiation Algorithms: A Comparative Study. Annales Geophysicae, 22: 2657-2668.

Kasten, F. 1996. Linke Turbidity Based on Improved Values of the Integral Rayleigh Optical Thickness. Solar Energy, 56: 239-244

Katz, M. Baille, A. and Mermier, M. 1982. Atmospheric Turbidity in a Semi –Rural Site – I: Evaluation and Comparison of Different Atmospheric Turbidity Coefficients. Solar Energy, 28(4): 323-327

Kondo, J. Nakamura, T. and Yamazaki. 1991. Estimation of the Solar and Downward Atmospheric Radiation. Tenki, 38: 41- 48

Marif, Y. Bechki, D. Zerrouk, M., Belhadj, MM. Bouguettaia, H. and Benmoussa. H. 2017. Estimation of Atmospheric Turbidity Over Adrar City in Algeria. Journal of King of Saud University, 17: 1317 - 1333

Marif, Y. Chiba, Y. Bilhadj, MM. Zerrouki, M. and Benhammou, M. 2018. A Clear Sky Irradiation Assessment Using a Modified Algerian Solar Atlas Model in Aldrar City. Energy reports, 4: 84 - 90

Muhammad, SU. Yahaya, DB. and Enaburekhan, JS. 2016. Estimating Atmospheric Precipitable Water from Common Variables. International Journal of Engineering Research and Technology, 5(2): 801-803.

Muhammad, SU. Yahaya, DB. and Enaburekhan, JS. 2016. Estimation of Mean Monthly Solar Radiation and Clearness Index. International Journal of Engineering Technology and Technology, 34 (1): 35-38

Oba, MD. Chendo, MAC. and Erusinfe, NE. 2016. Estimation of Angstrom Turbidity Coefficient Over Akoka. Nigerian Journal of Solar Energy, 27: 34-39

Ogunsola, OI. 1990. History of Energy Sources and Their Utilization in Nigeria. Energy Sources, 12(12): 181 – 198

Osueke, CO. and Ezugwu, CAK. 2011. Study of Nigerian Energy Resources and Its Consumption. International Journal of Scientific and Engineering Research, 2(12): 1 – 8

Power, HC. 2001. Estimating atmospheric Turbidity from Climate Data. Atmos. Env., 35(1): 125-134.

Scharmer, K. and Grief, J. 2000. European Solar Radiation Atlas (ESRA). Les Presses de l'Ecole des Mines de Paris, France